




## Article

# Transverse Oscillations of the M87 Jet Revealed by KaVA Observations

Hyunwook Ro <sup>1,2,\*</sup> , Kunwoo Yi <sup>3</sup>, Yuzhu Cui <sup>4,5</sup> , Motoki Kino <sup>6,7</sup>, Kazuhiro Hada <sup>8,9</sup> , Tomohisa Kawashima <sup>10</sup>, Yosuke Mizuno <sup>4,11,12</sup>, Bong Won Sohn <sup>1,2,13</sup> and Fumie Tazaki <sup>14</sup> 

<sup>1</sup> Department of Astronomy, Yonsei University, Yonsei-ro 50, Seodaemun-gu, Seoul 03722, Republic of Korea

<sup>2</sup> Korea Astronomy & Space Science Institute, Daedeokdae-ro 776, Yuseong-gu, Daejeon 34055, Republic of Korea

<sup>3</sup> Department of Physics and Astronomy, Seoul National University, Gwanak-gu, Seoul 08826, Republic of Korea

<sup>4</sup> Tsung-Dao Lee Institute, Shanghai Jiao Tong University, Shanghai 201210, China

<sup>5</sup> Research Center for Intelligent Computing Platforms, Zhejiang Laboratory, Hangzhou 311100, China

<sup>6</sup> Academic Support Center, Kogakuin University of Technology and Engineering, 2665-1 Nakano, Hachioji, Tokyo 192-0015, Japan

<sup>7</sup> National Astronomical Observatory of Japan, 2-21-1 Osawa, Mitaka, Tokyo 181-8588, Japan

<sup>8</sup> Mizusawa VLBI Observatory, National Astronomical Observatory of Japan, 2-12 Hoshigaoka, Mizusawa, Oshu, Iwate 023-0861, Japan

<sup>9</sup> Department of Astronomical Science, The Graduate University for Advanced Studies (SOKENDAI), 2-21-1 Osawa, Mitaka, Tokyo 181-8588, Japan

<sup>10</sup> Institute for Cosmic Ray Research, The University of Tokyo, 5-1-5 Kashiwanoha, Kashiwa, Chiba 277-8582, Japan

<sup>11</sup> School of Physics and Astronomy, Shanghai Jiao Tong University, Shanghai 200240, China

<sup>12</sup> Institut für Theoretische Physik, Goethe Universität, Max-von-Laue Str. 1, D-60438 Frankfurt am Main, Germany

<sup>13</sup> Department of Astronomy and Space Science, University of Science and Technology, Yuseong-gu, Daejeon 34113, Republic of Korea

<sup>14</sup> Tokyo Electron Technology Solutions Limited, Iwate 023-1101, Japan

\* Correspondence: hwro@yonsei.ac.kr



**Citation:** Ro, H.; Yi, K.; Cui, Y.; Kino, M.; Hada, K.; Kawashima, T.; Mizuno, Y.; Sohn, B.W.; Tazaki, F. Transverse Oscillations of the M87 Jet Revealed by KaVA Observations. *Galaxies* **2023**, *11*, 33. <https://doi.org/10.3390/galaxies11010033>

Academic Editor: Luigina Feretti

Received: 25 December 2022

Revised: 1 February 2023

Accepted: 6 February 2023

Published: 15 February 2023



**Copyright:** © 2023 by the authors. Licensee MDPI, Basel, Switzerland. This article is an open access article distributed under the terms and conditions of the Creative Commons Attribution (CC BY) license (<https://creativecommons.org/licenses/by/4.0/>).

**Abstract:** Recent VLBI monitoring has found transverse motions of the M87 jet. However, due to the limited cadence of previous observations, details of the transverse motion have not been fully revealed yet. We have regularly monitored the M87 jet at KVN and VERA Array (KaVA) 22 GHz from December 2013 to June 2016. The average time interval of the observation is  $\sim 0.1$  year, which is suitable for tracking short-term structural changes. From these observations, the M87 jet is well represented by double ridge lines in the region 2–12 mas from the core. We found that the ridge lines exhibit transverse oscillations in all observed regions with an average period of  $0.94 \pm 0.12$  years. When the sinusoidal fit is performed, we found that the amplitude of this oscillation is an order of  $\sim 0.1$  mas, and the oscillations in the northern and southern limbs are almost in phase. Considering the amplitude, it does not originate from Earth's parallax. We propose possible scenarios of the transverse oscillation, such as the propagation of jet instabilities or magneto-hydrodynamic (MHD) waves or perturbed mass injection around magnetically dominated accretion flows.

**Keywords:** active galactic nuclei (AGN); M87; relativistic jet; very long baseline interferometry (VLBI); oscillation; instability; accretion disk

## 1. Introduction

M87 is a giant elliptical galaxy at a distance of 16.8 Mpc [1], which harbors a super-massive black hole of  $M_{\bullet} = 6.5 \pm 0.7 \times 10^9 M_{\odot}$  [1] and a prominent jet that extends several kiloparsecs (kpc) away from the galaxy. At this distance, an angular size of 1 milli-arcsecond (mas) corresponds to  $\approx 0.081$  parsecs (pc)  $\approx 130$  Schwarzschild radius ( $r_s$ ), and a proper

motion of 1 mas/yr is equivalent to  $\sim 0.264c$ . It is, therefore, one of the best targets for studying the detailed structure of (sub)pc-scale jets and their evolution over time.

The launching region of the M87 jet is being intensively studied by Very Long Baseline Interferometry (VLBI), from which there is increasing evidence that the jet accelerates at distances less than  $\sim 10^6 r_s$  [2–5]. In addition, high-resolution VLBI observations investigated the edge-brightened structure of the M87 jet in the same region [6–10] and found that the M87 jet is collimating in a parabolic shape. The co-existence of acceleration and collimation in the M87 jet is as predicted from the magneto-hydrodynamic (MHD) acceleration model, e.g., [9,11–13].

#### *Transverse Motions in the Parsec-Scale Structures of the M87 Jet*

Several previous VLBI studies found that the pc-scale structure of the M87 jet exhibits transverse motions (i.e., the motion in the direction perpendicular to the jet axis). Walker et al. [10] have reported a quasi-periodic sideways shift in the M87 jet by analyzing roughly annual observations at a Very Long Baseline Array (VLBA), 43 GHz, over 17 years from 1999 to 2016. The jet shows a quasi-periodic sideways shift of about 8–10 years, and the shift propagates outward with a speed significantly slower than the flow speed. They concluded that the non-ballistic propagation speed of the long-term patterns is consistent with the propagation speed of the Kelvin–Helmholtz instability. Britzen et al. [14] have investigated the evolution of the ridge lines of the M87 jet using 31 VLBA observations at 15 GHz, spanning a time range between July 1995 and May 2011. They found that the M87 jet structures switch between two phases. In the first phase, the jet ridge lines are at least double, or the jet axis is displaced vertically. In the second phase, the jet ridge lines remain almost straight but smoothly curved, and the jet components are aligned along a jet axis. They suggested the transition period between the two phases is  $\sim 2$  years. They proposed the origin as a turbulent mass loading into the jet from the accretion disk.

Thus far, two different studies of the transverse motions of the M87 jet have been reported. However, the periods of transverse motions found in both studies are quite different from each other, even though they conducted observations over a long period of more than 15 years. This discrepancy means they are likely seeing different motions of the jets, implying that the transverse motions of the M87 jet may be more complex. However, both studies are limited in fully describing the transverse motions of the jet due to the low cadence and non-uniform spacing of the observations. Therefore, high-cadence monitoring with more regular time intervals is required to clearly understand the transverse motions in the M87 jet.

KaVA (KVN and VERA Array; [15]) has regularly observed M87 since late 2013. The major goal was to detect the velocity profile of the M87 accurately. The pilot observations of KaVA 22 GHz from December 2013 to June 2014 have successfully found superluminal motions in the region within 10 mas from the core [4]. A more complete picture of the jet acceleration profile was revealed with the biweekly observations in 2016 at 22 and 43 GHz [5]. KaVA monitoring of the M87 jet has the advantage of seeing the extended jet at shorter time intervals than the previous studies. In this work, we will use multi-epoch KaVA data to investigate the transverse motion of the M87 jet in detail. In Section 2, we describe the KaVA 22 GHz monitoring data from December 2013 to June 2016. Parts of these data were published in previous studies, and some are new in this study. In Section 3, we present a method for creating ridge lines in the jet and displaying the distribution of ridge lines for the M87 jet of all data. Section 4 analyzes the transverse motion of the M87 jet by fitting a sinusoidal curve and creating a periodogram. As a result, we found an oscillation with a period of  $\sim 1$  year at all distances of the jet. We propose possible origins of transverse oscillation in the M87 jet.

## **2. Observations**

We used KaVA 22 GHz observations from December 2013 to June 2016. Some of these data have already been published: 10 epochs from 5 December 2013 to 14 June 2014 in

Hada et al. [4], and 8 epochs of biweekly monitoring from 25 February 2016 to 13 June 2016 in Park et al. [5]. Data from 1 September 2014 to 16 May 2015 were newly added to this study after performing a standard data post-correlation process with the NRAO's Astronomical Image Processing System (AIPS; [16]). The detailed process is described by Park et al. [5]. During this process, the amplitude of data was multiplied by a factor of 1.35 for the data before 2015 May and 1.3 after 2015 May to correct for amplitude loss during correlation [17]. After that, imaging with CLEAN and self-calibration was performed using the Difmap software package [18]. When natural weighting is applied, the typical Full Width at Half Maximum (FWHM) of the synthesized beam is close to a circular shape with radii of 1.2 mas. We present naturally weighted CLEAN images for the data from 1 September 2014 to 16 May 2015 in Figure A1.

In total, we used 24 KaVA 22 GHz data to analyze the transverse motion. The image information for the data is summarized in Table A1. Due to the relatively short on-source time, the dynamic ranges for observations in 2013–2015 are relatively low compared to observations in 2016. However, it is possible to investigate jet structures up to  $\sim 12$  mas in almost all observations. Compared to the observations used in Walker et al. [10] and Britzen et al. [14], our KaVA 22 GHz monitoring is not a long period of observation ( $\sim 2.52$  years). However, due to its much shorter cadence (on average  $\sim 0.1$  year), it is suitable for studying the transverse oscillations of jets in more detail.

### 3. The Ridge Lines

The transverse motion of the M87 jet can be studied by tracking changes in the ridge lines. Various definitions of ridge lines of AGN jet have been used in previous studies, e.g., [14,19–22]. To obtain the ridge lines of the M87 jet, the following steps were taken, as summarized in Figure 1. Firstly, we restored all the maps to the same circular beam of  $1.2 \text{ mas} \times 1.2 \text{ mas}$ , which is the comparable size of the synthesized beam of KaVA at 22 GHz. Then, we rotated all images by  $-18$  degrees in order to align the jet's central axis with the horizontal axis, e.g., [10]. We then obtained one-dimensional brightness distributions perpendicular to the jet axis using the AIPS task *SLICE* for all successive steps of 0.2 mas down the jet starting at the core. The M87 jet shows a complex jet structure with a prominent limb-brightening; hence, there is usually more than one peak in the transverse brightness distribution, e.g., [8,10]. However, due to limited angular resolution, the transverse slice plots of our observations show a single peak up to a certain distance from the core and double peaks for the downstream jet. We fitted a single or double Gaussian to the transverse brightness distribution with the least squared method. Then, the ridge lines of the jet were derived by connecting the peaks of the Gaussian along the jet. We found that the boundary between single-ridge and double-ridge regions differs slightly from epoch to epoch depending on the data quality. However, from 2 mas from the core, the jet structure was sufficiently resolved into double ridges in all epochs. Therefore, in further analysis, we set the boundary as 2 mas for all epochs.

Figure 1 shows the ridge line of the M87 jet from one epoch of observation (25 February 2016). The bottom panels show transverse slice plots at 1.8, 2.4, 6.0, and 9.2 mas distance from the core. The solid black line is the transverse brightness distribution, and the solid blue and solid green lines are the single and double Gaussian fitting results, respectively. The error of the Gaussian peak intensity ( $\sigma_{\text{peak}}$ ), peak position ( $\sigma_{\text{position}}$ ) and size ( $\sigma_{\text{width}}$ ) is calculated using Equations (1)–(3) [23,24]:

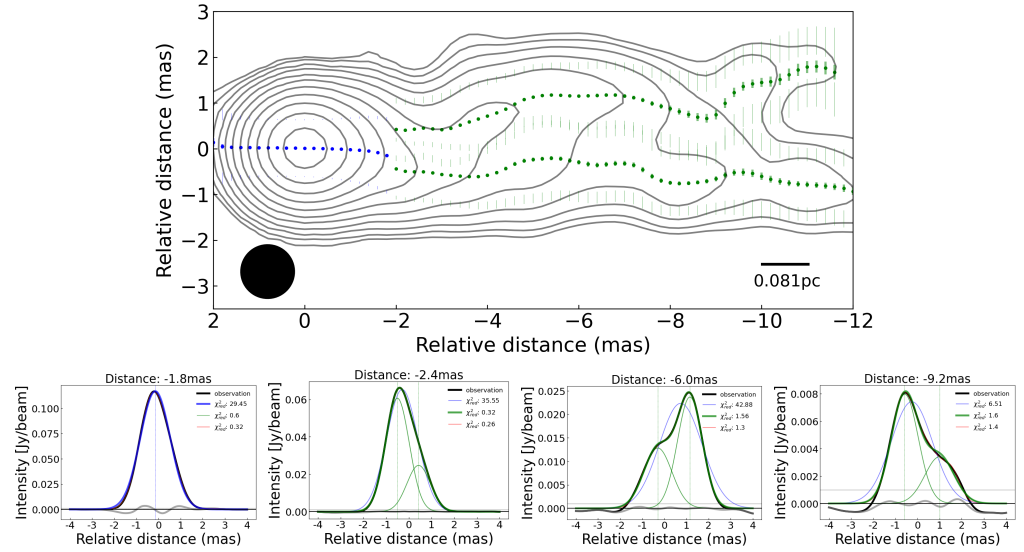


**Figure 1. (Top)** Example of the Gaussian model fitting results for drawing the ridge line of one epoch at the KaVA 22 GHz (25 February 2016). The image has been rotated by  $-18$  degrees. Contours start at  $3\sigma_{\text{rms}}$ , increasing in steps of 2. The black circle in the bottom left corner represents the size of the restoring beam, namely 1.2 mas circular Gaussian. **(Bottom)** Transverse brightness distributions at 4 different locations (at distances 1.8, 2.4, 6.0, 9.2 mas) and their Gaussian model fit results. The blue and green dots are the peak and FWHM positions of the best-fit results of single or double Gaussian models, respectively.

$$\sigma_{\text{peak}} = \sigma_{\text{rms}} \times \left(1 + \frac{S_{\text{peak}}}{\sigma_{\text{rms}}}\right)^{1/2} \quad (1)$$

$$\sigma_{\text{position}} = \sigma_{\text{peak}} \times \frac{d_{\text{FWHM}}}{2S_{\text{peak}}} \quad (2)$$

$$\sigma_{\text{width}} = 2\sigma_{\text{position}} \quad (3)$$

where  $\sigma_{\text{rms}}$  is the image rms noise,  $S_{\text{peak}}$  is the peak intensity of the Gaussian, and  $d_{\text{FWHM}}$  is the width of the Gaussian.

In the top panel, the positions of the Gaussian peaks are distributed as blue dots in the inner 2 mas from the core and as two green dots for more downstream. Errors in position are indicated by thick vertical lines. The Gaussian width is indicated by a thin vertical line, and the length of the line represents the error. It can be seen that the position and width of the Gaussian model are smoothly connected, confirming the good tracking of the jet structure.

Figure 2 shows the ridge lines of the M87 jet within 12 mas from the core from the KaVA 22 GHz observations between December 2013 to May 2014 (left panel), June 2014 to May 2015 (middle panel), and February 2016 to June 2016 (right panel), respectively. Contours represent the total intensity, starting at  $3\sigma_{\text{rms}}$  and increasing by a factor of two. Ridge lines that lie outside the contour lines or whose location changes abruptly are excluded. The observation date of each datum is written on the left of the contours. In general, the jet structures observed at KaVA 22 GHz are well represented by double ridge lines up to 12 mas from the core. The position error increases downstream. The northern limb tends to have shorter or more discontinuous ridge lines than the southern limb due to its weaker intensity.

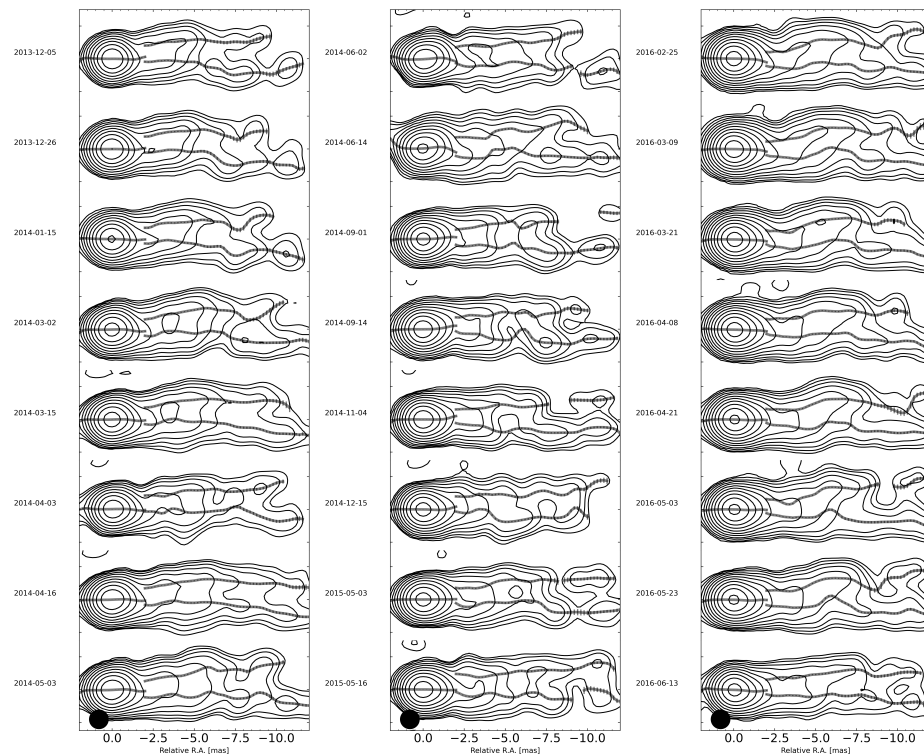


**Figure 2.** Ridge lines distribution of the M87 jet at 22 GHz from KaVA observations in December 2013 to May 2014 (**left**), June 2014 to May 2015 (**middle**), and February 2016 to June 2016 (**right**). The contours represent the total intensity. Contours start at  $3\sigma_{\text{rms}}$ , increasing in steps of 2. The  $\sigma_{\text{rms}}$  of each epoch is listed in Table A1. The black circles in the bottom left corner represent the size of the restoring beam, namely 1.2 mas circular Gaussian. All images have been rotated by  $-18$  degrees.

#### 4. Transverse Oscillation in the M87 Jet

To examine the transverse evolution of the jet structure, we traced the changes of the ridge lines with time in the transverse direction. The left panels of Figure 3 show the change in the transverse displacement of the ridge from the jet axis at distances of 1.8, 3.6, 5.4, and 6.8 mas. The 1.8 mas distance is in the single ridge region, and the rest are in the double ridge region. The transverse displacements of the northern ridge and southern ridge are expressed in red and blue dots, respectively. At all locations, the transverse position of the ridge line moves up and down as if oscillating with time.

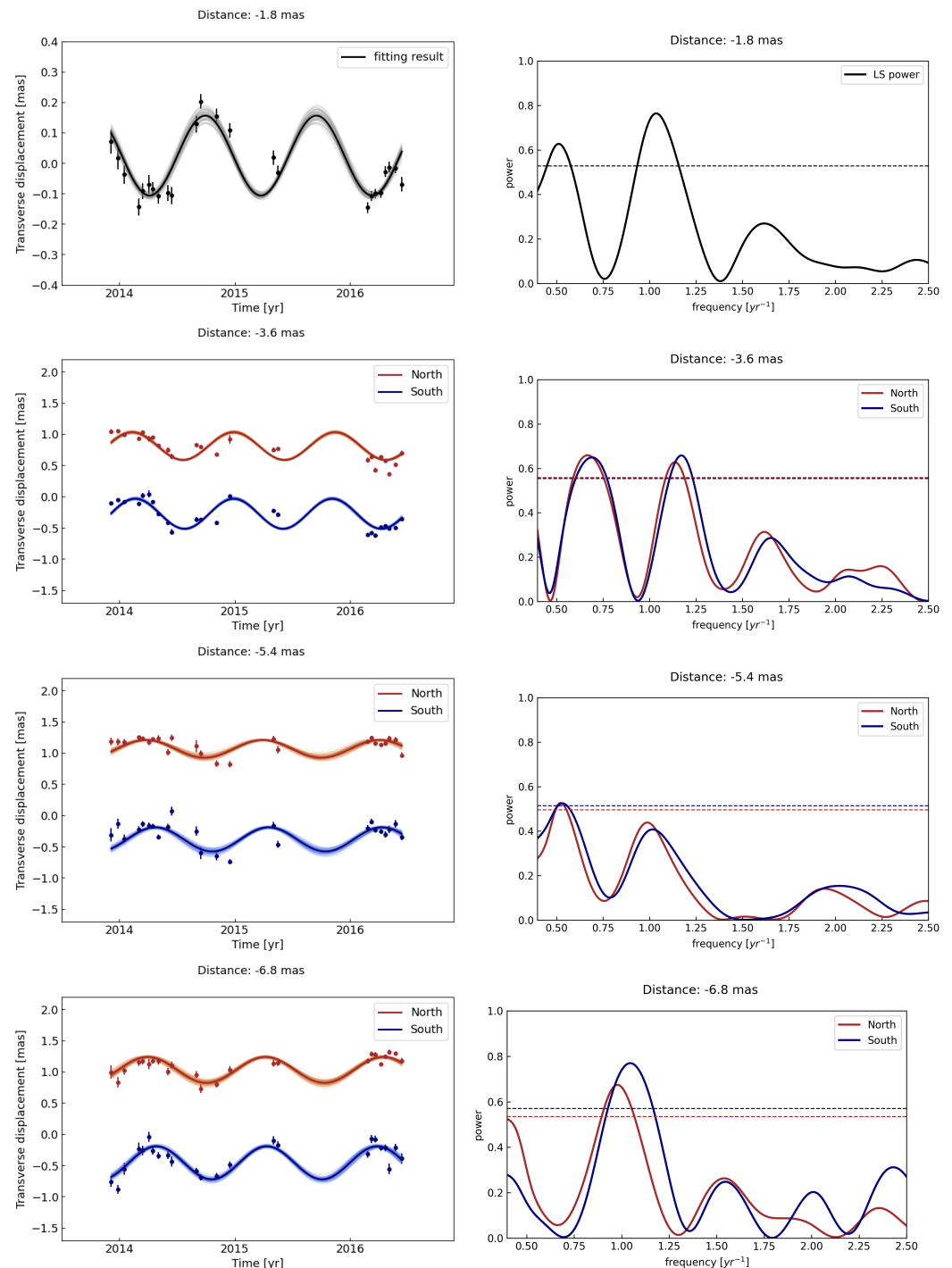
Several analyses were performed to investigate this transverse oscillatory motion. Firstly, we fitted the transverse displacement plot with a sinusoidal curve:

$$y = A \sin\left(\frac{2\pi}{P}t - \phi\right) + y_0 \quad (4)$$

where  $y$  is the transverse displacement,  $t$  is time,  $A$  is the amplitude,  $P$  is the period,  $\phi$  is the phase and  $y_0$  is the offset of the sinusoidal curve. We performed Markov Chain Monte Carlo (MCMC) method to find the best-fit result, e.g., [25]. The thick line in the left panels of Figure 3 is the best sinusoidal fit result. The thin lines are 100 randomly chosen model parameters from the MCMC samples to show the statistical errors. The best-fit parameters are summarized in Table 1. We found that the transverse motion of the jet is well described by a sinusoidal curve, meaning that the jet oscillates periodically. Figure 4 is the distribution of periods obtained by sinusoidal fitting to the transverse motion of the jet at all distances less than 12 mas at both ridges. The average of the distribution is 0.94 yr, and the standard deviation is 0.12 yr. This shows that the M87 oscillates transversely at all distances on both ridges with a similar period. We also found that the phase difference between the oscillations of the northern and southern limbs is less than one-tenth of the period. This means that the oscillations of the two ridges are



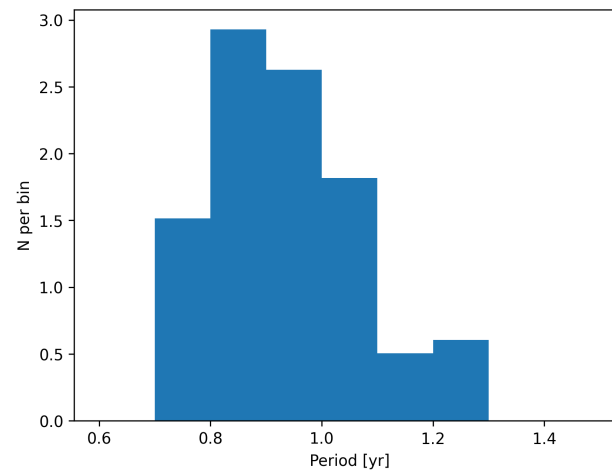
almost in phase. In Figure A2, we investigated whether the size of the restored beam could affect the sinusoidal fitting results, and found that the results are not changed.



**Figure 3.** (Left) Transverse oscillations of the M87 jet obtained at 1.8, 3.6, 5.4, and 6.8 mas from the core from December 2013 to June 2016. The filled circle is the transverse displacement of the jet ridge from the jet axis. The thick line is the best-fit sinusoidal model. The thin lines are 100 randomly chosen model parameters from the MCMC samples to show the statistical errors. The black line is the result of the single ridge and the red and blue lines are the result of the northern and southern ridges, respectively. The amplitude ( $A$ ), period ( $P$ ), phase ( $\phi$ ), and offset ( $y_0$ ) of the sinusoidal fit are summarized in Table 1. (Right) Lomb–Scargle periodogram results of the transverse oscillations of the M87 jet at the same locations. The dashed horizontal line is the false alarm probability of 10% with an assumption of white noise.

**Table 1.** Summary of sinusoidal fit results for the transverse motion of the M87 jet at a distance of 1.8, 3.6, 5.4, and 6.8.

Distance	1.8 mas	3.6 mas	5.4 mas	6.8 mas
$A$ (mas)	$0.131 \pm 0.008$	$0.223 \pm 0.010$	$0.143 \pm 0.017$	$0.207 \pm 0.019$
$P$ (yr)	$0.966 \pm 0.010$	$0.880 \pm 0.005$	$1.013 \pm 0.020$	$1.023 \pm 0.017$
$\phi$ (rad)	$3.742 \pm 0.105$	$6.019 \pm 0.064$	$0.302 \pm 0.166$	$0.371 \pm 0.198$
$y_0$ (mas)	$0.025 \pm 0.007$	$0.808 \pm 0.007$	$1.064 \pm 0.015$	$1.029 \pm 0.015$
$A$ (mas)	-	$0.241 \pm 0.010$	$0.194 \pm 0.020$	$0.264 \pm 0.017$
$P$ (yr)	-	$0.854 \pm 0.004$	$0.983 \pm 0.018$	$0.958 \pm 0.014$
$\phi$ (rad)	-	$6.256 \pm 0.064$	$0.878 \pm 0.168$	$1.006 \pm 0.147$
$y_0$ (mas)	-	$-0.275 \pm 0.007$	$-0.384 \pm 0.017$	$-0.459 \pm 0.015$

**Figure 4.** Distribution of period of the transverse oscillations obtained from sinusoidal fit at all distances less than 12 mas. The average period is 0.94 yr, and the standard deviation is 0.12 yr.

We also performed Lomb–Scargle periodogram analysis for each transverse oscillation plot [26,27]. We evaluate the periodogram power at frequencies between  $f_{\min} = 1/T$ , where  $T$  is the total time of the observations and  $f_{\max} = 1/(2T_{\min})$ , corresponding to one over twice the minimum time interval between observations [28]. The number of grids in the frequency range was set to 2000 in order to sufficiently sample at every period. The results of the periodogram analyses at each distance are shown in the right panels of Figure 3. We found that the periodogram shows a strong peak at a similar place as the value obtained from the sinusoidal fit. We also found another peak at a lower frequency, and the power of this low-frequency peak is similar or slightly stronger than the high-frequency peak at 3.6 and 5.4 mas. However, the position of the low-frequency peak changes with distance and even disappears at 6.8 mas. Therefore, it is not caused by the oscillations inside the jet and may be an artifact caused by the non-uniform time interval of the observations, e.g., [28]. Further observations may clarify the presence of the low-frequency peak. The horizontal line stands for the false-alarm probability (i.e., the probability that a signal with no periodic component would lead to a peak of this magnitude) of 10% with an assumption of white noise <sup>1</sup> [28]. This shows that the probability of which the periodic signal originated from the random component is less than 10% except at 5.4 mas.

From these analyses, we were able to reveal transverse oscillations of the M87 jet at all distances with an average period of  $0.94 \pm 0.12$  year. This fast and periodic oscillation in the M87 jet has never been reported in previous studies. The period is much shorter than the quasi-periodic sideways shifts reported by Walker et al. [10] (8–10 years). It is relatively similar to the timescale of the transition of the jet structures reported by Britzen et al. [14] ( $\sim 2$  years), but still about half of it. Therefore, it is possible that either we discovered a totally new type of oscillation with a much faster period or more clearly revealed oscillations that previous studies could not fully track due to their insufficient time sampling.

### *Origins of the Transverse Oscillations*

Given that the period of the oscillations is about one year, it is a natural question whether the oscillation originates from the projection effect of the Earth's revolution. However, the parallax angle of the M87 is  $\sim 0.1 \mu\text{as}$ , which is 1000 times smaller than the observed oscillation amplitude ( $\sim 0.1 \text{ mas}$ ). Thus, we can rule out the possibility that the observed oscillations originate from Earth's parallax. Future observations are able to test this possibility, as the Earth's revolution predicts perfectly periodic oscillations with an exactly one-year period.

Several jet-intrinsic origins can be proposed to explain transverse oscillations in the M87 jet. Advection of the distorted jet structure created by magneto-hydrodynamic (MHD) instabilities is one of the possible scenarios, e.g., [29]. Several previous studies have suggested Kelvin–Helmholtz instability (KHI) to describe the M87 jet's twisted filament structures, which are shown up to kpc-scales, e.g., [30–32]. Walker et al. [10] explained the long-term sideways shifts observed in pc-scale jets as the propagation of a helical pattern created by KHI along the jet. However, it is unclear whether the newly discovered fast oscillation can be described by KHI, as the region observed by KaVA may be highly magnetized, e.g., [33]. Rather, current-driven instability (CDI) such as sausage instability ( $m = 0$ ) or kink instability ( $m = 1$ ) can cause oscillations in the magnetically dominated regions e.g., [34–36].

For a highly magnetized jet, the propagation of transverse MHD waves (i.e., Alfvén waves) is another possible scenario to explain the transverse oscillation [21]. This scenario requires a source to excite the wave upstream of the jet, in analogy to exciting a wave on a whip by shaking the handle, and the jet's magnetic field strength and mass density determine the speed of wave propagation.

Alternatively, MHD simulations of the magnetically arrested disk (MAD) have shown that oscillations in the energy outflow of the jet could be induced by the accumulation and escape of magnetic field line bundles in the innermost part of accretion disks [37,38]. According to this scenario, multiple harmonics of the quasi-periodic oscillations in the jet are expected [38]. Future observations can test this scenario by looking for the additional oscillations in the jet.

## 5. Summary

In this work, we found a transverse oscillation of the M87 jet with an average period of  $0.94 \pm 0.12$  years using high-cadence monitoring observations of KaVA at 22 GHz. It has a much shorter period than that reported in previous studies. Therefore, it may be a new type of oscillation that has never been reported or is not clearly seen in previous observations due to insufficient time intervals. The oscillation has almost the same period at all positions of the jet and has an amplitude of about  $\sim 0.1 \text{ mas}$ . The amplitude of the oscillation is about 1000 times larger than the amplitude expected from Earth's parallax ( $\sim 0.1 \mu\text{as}$ ), which excludes the possibility that this oscillation originated from the Earth revolution. We found that the oscillations were present in both the north and south limbs in nearly the same phase. We proposed that the propagation of jet instability or perturbed mass accretion occurred in the magnetically arrested disks as possible origins.

Since 2017, KaVA has expanded as EAVN (East Asia VLBI Network; [39]) by joining Chinese telescopes. EAVN monitoring is currently the only monitoring that steadily observes the M87 jet. Using these observations, we will investigate the transverse oscillations in the M87 jet in more detail.

**Author Contributions:** Conceptualization, H.R., M.K. and K.H.; methodology, H.R., M.K. and K.H.; software, H.R.; validation, H.R., K.Y. and Y.C.; formal analysis, H.R.; data curation, H.R., K.Y., Y.C. and K.H.; writing—original draft, H.R.; writing—review and editing, K.Y., Y.C., M.K., K.H., T.K., Y.M., B.W.S. and F.T.; visualization, H.R.; supervision, M.K. and B.W.S.; project administration, M.K. and B.W.S.; funding acquisition, B.W.S. All authors have read and agreed to the published version of the manuscript.



**Funding:** This research was supported by the Korea Astronomy and Space Science Institute under the R&D program supervised by the Ministry of Science and ICT. H.R. and B.W.S. acknowledge support from the KASI-Yonsei DRC program of the Korea Research Council of Fundamental Science and Technology (DRC-12-2-KASI). Y.C. is supported by the China Postdoctoral Science Foundation (2022M712084). And just in case, please also make sure my grant no. is 2022M712084. Y.M. is supported by the National Natural Science Foundation of China (12273022) and the Shanghai pilot program of international scientists for basic research (22JC1410600).

**Data Availability Statement:** All observing data obtained by KaVA, except the data in the term of the right of occupation by a principal investigator, are archived via the following website. <https://radio.kasi.re.kr/arch/search.php> (accessed on 5 February 2023).

**Acknowledgments:** This work is based on observations made with the KaVA, which is operated by the Korea Astronomy and Space Science Institute and the National Astronomical Observatory of Japan.

**Conflicts of Interest:** The authors declare no conflict of interest.

#### Appendix A. Image Information of KaVA 22 GHz Monitoring of the M87 Jet from December 2013 to June 2016

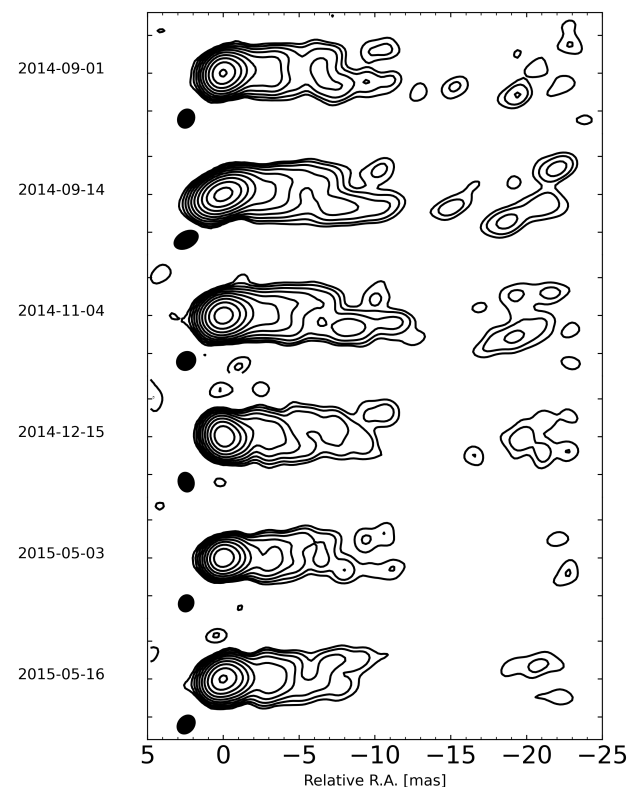


**Figure A1.** Total intensity maps of KaVA 22 GHz observations of the M87 jet between September 01 2014 and May 16 2015. Contours start at  $3\sigma_{\text{rms}}$ , increasing in steps of 2. The synthesized beam for individual epochs is drawn as a black ellipse on the bottom left side of the individual maps.

**Table A1.** Summary of KaVA 22 GHz observations of the M87 jet from December 2013 to June 2016.

Obs. Date (1)	Beam Size (mas × mas, deg) (2)	$I_{\text{peak}}$ (Jy/beam) (3)	$\sigma_{\text{rms}}$ (mJy/beam) (4)	Dynamic Range (5)
5 December 2013	$1.31 \times 1.14, -18.0$	1.67	1.003	1669
26 December 2013	$1.61 \times 1.23, -42.7$	1.32	0.784	1688
15 January 2014	$1.83 \times 1.51, -54.3$	1.36	0.76	1794
2 March 2014	$1.50 \times 1.21, 3.0$	1.39	0.516	2695
15 March 2014	$1.34 \times 1.14, -15.9$	1.42	0.464	3055
3 April 2014	$1.32 \times 1.22, 14.5$	1.35	0.775	1742
16 April 2014	$1.27 \times 1.10, -17.7$	1.39	0.37	3758
3 May 2014	$1.47 \times 1.26, 11.8$	1.42	0.386	3672
2 June 2014	$1.08 \times 0.91, -18.3$	1.17	0.734	1600
14 June 2014	$1.34 \times 1.10, -11.5$	1.11	0.531	2085
1 September 2014	$1.35 \times 1.16, -7.9$	1.27	0.627	2024
14 September 2014	$1.56 \times 1.15, -41.3$	1.28	0.497	2580
4 November 2014	$1.41 \times 1.26, -32.2$	1.32	0.491	2695
15 December 2014	$1.27 \times 1.10, 2.34$	0.92	0.442	2077
3 May 2015	$1.22 \times 1.08, -4.1$	1.25	0.603	2070
16 May 2015	$1.42 \times 1.15, -21.5$	1.26	0.515	2448
25 February 2016	$1.31 \times 1.15, -5.9$	1.42	0.289	4903
9 March 2016	$1.38 \times 1.15, -2.3$	1.35	0.247	5474
21 March 2016	$1.55 \times 1.26, -14.9$	1.40	0.291	4825
8 April 2016	$1.36 \times 1.12, 1.9$	1.27	0.287	4439
21 April 2016	$1.28 \times 1.16, -3.7$	1.29	0.357	3605
3 May 2016	$1.30 \times 1.05, -11.9$	1.07	0.281	3794
23 May 2016	$1.24 \times 1.08, -12.6$	1.12	0.303	3690
13 June 2016	$1.26 \times 1.14, 5.3$	0.79	0.394	2013

NOTE—(1) Observation date. (2) Synthesized beam size with a natural weighting scheme. (3) Peak intensity of the image with a natural weighting scheme. (4) Image rms noise ( $\sigma_{\text{rms}}$ ) with a natural weighting scheme. (5) Dynamic range of the image calculated from  $I_{\text{peak}}/\sigma_{\text{rms}}$ .

## Appendix B. Effect of the Restoring Beam Size

In this work, we used the restoring beam of  $1.2 \times 1.2$  mas while making ridge lines. However, since the separation between the northern limb and the southern limb is not significant, the choice of the restoring beam size could affect the oscillation analysis. Figure A2 summarizes the transverse motion of the ridge lines and the sinusoidal fitting results obtained using different restoring beams at distances of 1.8, 3.6, 5.4 and 6.8 mas. Different colors represent different beam sizes, including smaller ( $1.0 \times 1.0$  mas) and larger ( $1.5 \times 1.5$  mas) beams. From these experiments, we found that the size of the restoring beam does not affect the oscillation period, while there are some differences in amplitude, especially in the upstream region where the gap between the northern and southern ridge is smaller. It confirms that the main conclusion of this study is not affected by the beam size.

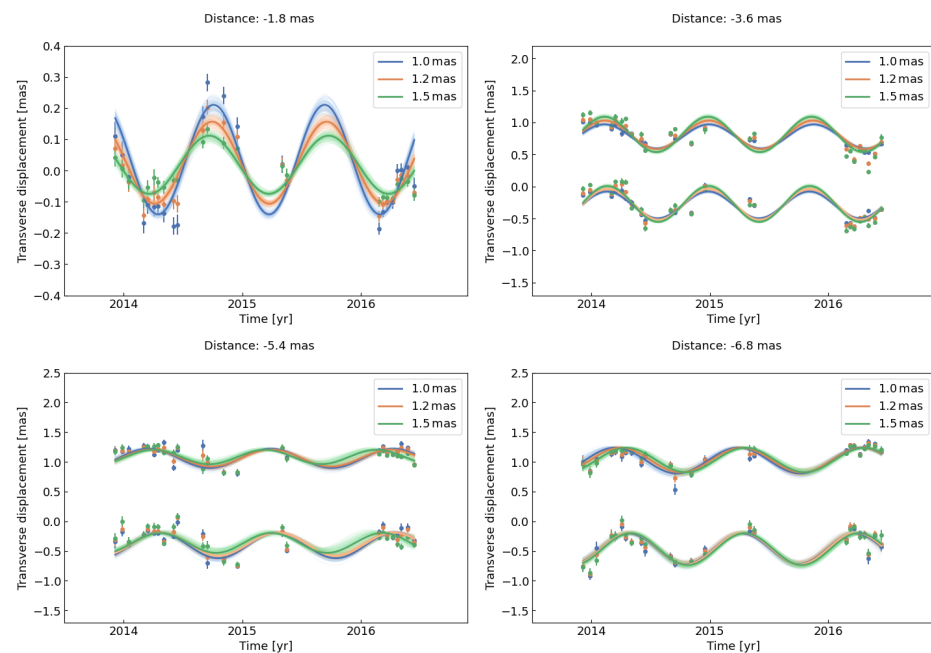


**Figure A2.** Transverse oscillations of the M87 jet, obtained at distances of 1.8, 3.6, 5.4, and 6.8 mas by applying different sizes of restoring beams. The blue, orange, and green dots represent the transverse displacement of the ridge lines obtained by applying circular restoring beams with a radius of 1.0, 1.2, and 1.5 mas, respectively, and the solid lines are their sinusoidal fitting results. At all distances, the oscillation period is almost unchanged with respect to the beam size, while the amplitude is slightly different.

## Notes

- <sup>1</sup> That is, the power of the random component in the periodogram is constant with respect to the frequency. In many situations of interest, however, this assumption does not hold. For more discussions, see VanderPlas [28] and references therein.

## References

1. Event Horizon Telescope Collaboration; Akiyama, K.; Alberdi, A.; Alef, W.; Asada, K.; Azulay, R.; Bacsko, A.K.; Ball, D.; Baloković, M.; Barrett, J.; et al. First M87 Event Horizon Telescope Results. I. The Shadow of the Supermassive Black Hole. *Astrophys. J. Lett.* **2019**, *875*, L1. [\[CrossRef\]](#)
2. Asada, K.; Nakamura, M.; Doi, A.; Nagai, H.; Inoue, M. Discovery of Sub- to Superluminal Motions in the M87 Jet: An Implication of Acceleration from Sub-relativistic to Relativistic Speeds. *Astrophys. J. Lett.* **2014**, *781*, L2. [\[CrossRef\]](#)
3. Mertens, F.; Lobanov, A.P.; Walker, R.C.; Hardee, P.E. Kinematics of the jet in M 87 on scales of 100–1000 Schwarzschild radii. *Astron. Astrophys.* **2016**, *595*, A54. [\[CrossRef\]](#)
4. Hada, K.; Park, J.H.; Kino, M.; Niinuma, K.; Sohn, B.W.; Ro, H.W.; Jung, T.; Algaba, J.C.; Zhao, G.Y.; Lee, S.S.; et al. Pilot KaVA monitoring on the M 87 jet: Confirming the inner jet structure and superluminal motions at sub-pc scales. *Publ. Astron. Soc. Jpn.* **2017**, *69*, 71. [\[CrossRef\]](#)
5. Park, J.; Hada, K.; Kino, M.; Nakamura, M.; Hodgson, J.; Ro, H.; Cui, Y.; Asada, K.; Algaba, J.C.; Sawada-Satoh, S.; et al. Kinematics of the M87 Jet in the Collimation Zone: Gradual Acceleration and Velocity Stratification. *Astrophys. J.* **2019**, *887*, 147. [\[CrossRef\]](#)
6. Asada, K.; Nakamura, M. The Structure of the M87 Jet: A Transition from Parabolic to Conical Streamlines. *Astrophys. J. Lett.* **2012**, *745*, L28. [\[CrossRef\]](#)
7. Hada, K.; Kino, M.; Doi, A.; Nagai, H.; Honma, M.; Akiyama, K.; Tazaki, F.; Lico, R.; Giroletti, M.; Giovannini, G.; et al. High-sensitivity 86 GHz (3.5 mm) VLBI Observations of M87: Deep Imaging of the Jet Base at a Resolution of 10 Schwarzschild Radii. *Astrophys. J.* **2016**, *817*, 131. [\[CrossRef\]](#)
8. Kim, J.Y.; Krichbaum, T.P.; Lu, R.S.; Ros, E.; Bach, U.; Bremer, M.; de Vicente, P.; Lindqvist, M.; Zensus, J.A. The limb-brightened jet of M87 down to the 7 Schwarzschild radii scale. *Astron. Astrophys.* **2018**, *616*, A188. [\[CrossRef\]](#)
9. Nakamura, M.; Asada, K.; Hada, K.; Pu, H.Y.; Noble, S.; Tseng, C.; Toma, K.; Kino, M.; Nagai, H.; Takahashi, K.; et al. Parabolic Jets from the Spinning Black Hole in M87. *Astrophys. J.* **2018**, *868*, 146. [\[CrossRef\]](#)
10. Walker, R.C.; Hardee, P.E.; Davies, F.B.; Ly, C.; Junor, W. The Structure and Dynamics of the Subparsec Jet in M87 Based on 50 VLBA Observations over 17 Years at 43 GHz. *Astrophys. J.* **2018**, *855*, 128. [\[CrossRef\]](#)

11. McKinney, J.C. General relativistic magnetohydrodynamic simulations of the jet formation and large-scale propagation from black hole accretion systems. *Mon. Not. R. Astron. Soc.* **2006**, *368*, 1561–1582. [\[CrossRef\]](#)
12. Komissarov, S.S.; Barkov, M.V.; Vlahakis, N.; Königl, A. Magnetic acceleration of relativistic active galactic nucleus jets. *Mon. Not. R. Astron. Soc.* **2007**, *380*, 51–70. [\[CrossRef\]](#)
13. Chatterjee, K.; Liska, M.; Tchekhovskoy, A.; Markoff, S.B. Accelerating AGN jets to parsec scales using general relativistic MHD simulations. *Mon. Not. R. Astron. Soc.* **2019**, *490*, 2200–2218. [\[CrossRef\]](#)
14. Britzen, S.; Fendt, C.; Eckart, A.; Karas, V. A new view on the M 87 jet origin: Turbulent loading leading to large-scale episodic wiggling. *Astron. Astrophys.* **2017**, *601*, A52. [\[CrossRef\]](#)
15. Niinuma, K.; Lee, S.S.; Kino, M.; Sohn, B.W.; Akiyama, K.; Zhao, G.Y.; Sawada-Sato, S.; Trippe, S.; Hada, K.; Jung, T.; et al. VLBI observations of bright AGN jets with the KVN and VERA Array (KaVA): Evaluation of imaging capability. *Publ. Astron. Soc. Jpn.* **2014**, *66*, 103. [\[CrossRef\]](#)
16. Greisen, E.W. AIPS, the VLA, and the VLBA. In *Information Handling in Astronomy-Historical Vistas*; Heck, A., Ed.; Springer: Dordrecht, The Netherlands, 2003; Volume 285, p. 109. [\[CrossRef\]](#)
17. Lee, S.S.; Byun, D.Y.; Oh, C.S.; Kim, H.R.; Kim, J.; Jung, T.; Oh, S.J.; Roh, D.G.; Jung, D.K.; Yeom, J.H. Amplitude Correction Factors of Korean VLBI Network Observations. *J. Korean Astron. Soc.* **2015**, *48*, 229–236. [\[CrossRef\]](#)
18. Shepherd, M.C. Difmap: An Interactive Program for Synthesis Imaging. In *Proceedings of the Astronomical Data Analysis Software and Systems VI*; Astronomical Society of the Pacific Conference Series; Hunt, G.; Payne, H., Eds.; Astronomical Society of the Pacific: San Francisco, CA, USA, 1997; Volume 125, p. 77.
19. Perucho, M.; Kovalev, Y.Y.; Lobanov, A.P.; Hardee, P.E.; Agudo, I. Anatomy of Helical Extragalactic Jets: The Case of S5 0836+710. *Astrophys. J.* **2012**, *749*, 55. [\[CrossRef\]](#)
20. Fromm, C.M.; Ros, E.; Perucho, M.; Savolainen, T.; Mimica, P.; Kadler, M.; Lobanov, A.P.; Zensus, J.A. Catching the radio flare in CTA 102. III. Core-shift and spectral analysis. *Astron. Astrophys.* **2013**, *557*, A105. [\[CrossRef\]](#)
21. Cohen, M.H.; Meier, D.L.; Arshakian, T.G.; Clausen-Brown, E.; Homan, D.C.; Hovatta, T.; Kovalev, Y.Y.; Lister, M.L.; Pushkarev, A.B.; Richards, J.L.; et al. Studies of the Jet in BL Lacertae. II. Superluminal Alfvén Waves. *Astrophys. J.* **2015**, *803*, 3. [\[CrossRef\]](#)
22. Pushkarev, A.B.; Kovalev, Y.Y.; Lister, M.L.; Savolainen, T. MOJAVE-XIV. Shapes and opening angles of AGN jets. *Mon. Not. R. Astron. Soc.* **2017**, *468*, 4992–5003. [\[CrossRef\]](#)
23. Fomalont, E.B. Image Analysis. In *Proceedings of the Synthesis Imaging in Radio Astronomy II*; Astronomical Society of the Pacific Conference Series; Taylor, G.B., Carilli, C.L., Perley, R.A., Eds.; Astronomical Society of the Pacific: San Francisco, CA, USA, 1999; Volume 180, p. 301.
24. Lee, S.S.; Lobanov, A.P.; Krichbaum, T.P.; Witzel, A.; Zensus, A.; Bremer, M.; Greve, A.; Grewing, M. A Global 86 GHz VLBI Survey of Compact Radio Sources. *Astron. J.* **2008**, *136*, 159–180. [\[CrossRef\]](#)
25. Hogg, D.W.; Foreman-Mackey, D. Data Analysis Recipes: Using Markov Chain Monte Carlo. *Astrophys. J. Suppl. Ser.* **2018**, *236*, 11. [\[CrossRef\]](#)
26. Lomb, N.R. Least-Squares Frequency Analysis of Unequally Spaced Data. *Astrophys. Space Sci.* **1976**, *39*, 447–462. [\[CrossRef\]](#)
27. Scargle, J.D. Studies in astronomical time series analysis. II. Statistical aspects of spectral analysis of unevenly spaced data. *Astrophys. J.* **1982**, *263*, 835–853. [\[CrossRef\]](#)
28. VanderPlas, J.T. Understanding the Lomb-Scargle Periodogram. *Astrophys. J. Suppl. Ser.* **2018**, *236*, 16. [\[CrossRef\]](#)
29. Hardee, P.E. The stability of astrophysical jets. In *Proceedings of the Jets at All Scales*; Romero, G.E., Sunyaev, R.A., Belloni, T., Eds.; Cambridge University Press & Assessment: Cambridge, UK, 2011; Volume 275, pp. 41–49. [\[CrossRef\]](#)
30. Lobanov, A.; Hardee, P.; Eilek, J. Internal structure and dynamics of the kiloparsec-scale jet in M87. *New Astron. Rev.* **2003**, *47*, 629–632. [\[CrossRef\]](#)
31. Hardee, P.E.; Eilek, J.A. Using Twisted Filaments to Model the Inner Jet in M 87. *Astrophys. J.* **2011**, *735*, 61. [\[CrossRef\]](#)
32. Pasetto, A.; Carrasco-González, C.; Gómez, J.L.; Martí, J.M.; Perucho, M.; O’Sullivan, S.P.; Anderson, C.; Díaz-González, D.J.; Fuentes, A.; Wardle, J. Reading M87’s DNA: A Double Helix Revealing a Large-scale Helical Magnetic Field. *Astrophys. J. Lett.* **2021**, *923*, L5. [\[CrossRef\]](#)
33. Kino, M.; Takahara, F.; Hada, K.; Akiyama, K.; Nagai, H.; Sohn, B.W. Magnetization Degree at the Jet Base of M87 Derived from the Event Horizon Telescope Data: Testing the Magnetically Driven Jet Paradigm. *Astrophys. J.* **2015**, *803*, 30. [\[CrossRef\]](#)
34. Mizuno, Y.; Lyubarsky, Y.; Nishikawa, K.I.; Hardee, P.E. Three-Dimensional Relativistic Magnetohydrodynamic Simulations of Current-Driven Instability. I. Instability of a Static Column. *Astrophys. J.* **2009**, *700*, 684–693. [\[CrossRef\]](#)
35. Singh, C.B.; Mizuno, Y.; de Gouveia Dal Pino, E.M. Spatial Growth of Current-driven Instability in Relativistic Rotating Jets and the Search for Magnetic Reconnection. *Astrophys. J.* **2016**, *824*, 48. [\[CrossRef\]](#)
36. Dong, L.; Zhang, H.; Giannios, D. Kink instabilities in relativistic jets can drive quasi-periodic radiation signatures. *Mon. Not. R. Astron. Soc.* **2020**, *494*, 1817–1825. [\[CrossRef\]](#)
37. Tchekhovskoy, A.; Narayan, R.; McKinney, J.C. Efficient generation of jets from magnetically arrested accretion on a rapidly spinning black hole. *Mon. Not. R. Astron. Soc.* **2011**, *418*, L79–L83. [\[CrossRef\]](#)

38. McKinney, J.C.; Tchekhovskoy, A.; Blandford, R.D. General relativistic magnetohydrodynamic simulations of magnetically choked accretion flows around black holes. *Mon. Not. R. Astron. Soc.* **2012**, *423*, 3083–3117. [[CrossRef](#)]
39. Cui, Y.Z.; Hada, K.; Kino, M.; Sohn, B.W.; Park, J.; Ro, H.W.; Sawada-Satoh, S.; Jiang, W.; Cui, L.; Honma, M.; et al. East Asian VLBI Network observations of active galactic nuclei jets: Imaging with KaVA+Tianma+Nanshan. *Res. Astron. Astrophys.* **2021**, *21*, 205. [[CrossRef](#)]

**Disclaimer/Publisher’s Note:** The statements, opinions and data contained in all publications are solely those of the individual author(s) and contributor(s) and not of MDPI and/or the editor(s). MDPI and/or the editor(s) disclaim responsibility for any injury to people or property resulting from any ideas, methods, instructions or products referred to in the content.